Journal of Applied Mathematics and Mechanics 74 (2010) 204–213

Contents lists available at ScienceDirect

Journal of Applied Mathematics and Mechanics

journal homepage: www.elsevier.com/locate/jappmathmech

Corrugation of a flexible ring under external hydrostatic compression☆

D.V. Dolgikh, V.V. Kiselev

Ekaterinburg, Russia

ARTICLE INFO

Article history:
Received 21 July 2008

ABSTRACT

The initial non-linearly elastic stage of a change in the shape of thin flexible ring under an external hydrostatic pressure is described. At this stage, the formation of alternating bulges and hollows in the ring in a circular direction is due to the balance of non-linearity and dispersion effects. A model is proposed which enables the dependence of the curvature of the deformed ring on the external pressure to be obtained. The shape of the ring is established from the known curvature by methods of differential geometry. Possible types of corrugation of the initial circular ring are obtained. The change in the shape of the ring around a rigid rod, placed inside the ring, is described. The strict relation between the amplitude of the bulges and hollows in the circumferential direction of the ring also prevents the formation of rigid edges on its surface.

The possibility of controlling the development of local instabilities of hydrostatically compressed shells has been investigated experimentally.[1,2] Ranges of the degrees of deformation of the material, the external pressure and the geometrical parameters of the shells, for which initially circular shells acquire the shape of the cross-section (circular, square, or any "serrated" shape), specified by rigid couplings, were obtained. It is important that, after a change in the shape of the shell, there are extended parts along the generatrix with an unchanged cross-section. In order to approximate to a theoretical description of the problem, a cylindrical shell is considered, the length of which is somewhat greater than the radius of its mean surface, so that the stress distribution at a sufficient distance from the ends does not change along the generatrix. It then follows from symmetry considerations that any initial plane cross-section of the shell remains plane and, consequently, the longitudinal deformation of the middle part of the shell is the same at each stage of the change in shape of its cross-section.[3,4] In this case, the representation of the nature of the corrugation of the cross-section of the shell can give rise to the problem of the change in the shape of an initially circular ring of unit height.

In this formulation, the equations defining the non-linearly elastic bending of a thin ring are identical with the equations characterising the change in the shape of a flexible rod, whose axis always lies in a single plane. Beginning with Euler's work, the theory of rods serves as the standard for the solution of boundary-value problems for elastic systems with a specified load, the consideration of problems of the stability of these solutions, and also the search for criteria, on the basis of which, among the several forms of equilibrium of the system, one must choose the form observed experimentally.

It is worth recalling some results of the theory of rods that are useful when discussing problems of the deformation of a ring.

It is well known that some forms of rods may change into others when the external stresses change. Although some forms of equilibrium of rods or rings are unstable, they can be stabilized by introducing appropriate strengthening constraints.[5] It is precisely this approach that is used[1,2] to control the deformation of shells. The most widely used approach when analysing the loss in shape of loaded rods is to consider the possible static equilibria of rods and to investigate the bifurcations between them using energy variational principles (see Refs 4 and 5 and the references given there).

For rapid longitudinal loading of a rod, when the rate of increase of the compressing force is fairly high, its elements are unable to move in a direction normal to the rod axis. Because of this, the compressing force may reach the first critical value and even considerably exceed it earlier than the bendings reach considerable values. Since, in this dynamic process, the compressing force may not only exceed the first but even higher critical values, we must expect the appearance of higher forms of loss of stability. This possibility was described for the first time for rods and rings in Ref. 6 within the framework of the non-linear theory of elasticity. A rod was subjected to the action of a suddenly applied force, which then remained constant (in general, the time taken for the load to increase must be less than the relaxation

☆ *Prikl. Mat. Mekh*. Vol. 74, No. 2, pp. 285–298, 2010.

E-mail addresses: dolgihd@imp.uran.ru (D.V. Dolgikh), kiseliev@imp.uran.ru (V.V. Kiselev).

0021-8928/$ – see front matter
doi:10.1016/j.jappmathmech.2010.05.011

time of the system). To determine the observed shapes of the rod, a dynamic criterion of stability was used, which was as follows. The initial bending of the rod was expanded in a Fourier series in forms of the static loss of stability. It was assumed that a rod shape is obtained, the amplitude of variation of which possesses the greatest rate of increase for a given load. On the surfaces of hydrostatically compressed shells, a different number of bulges and depressions is also observed depending on their geometrical and material parameters, as well as the value of the external pressure.[1,2,5]

For heavy loads, local bendings of a ring or rod are determined by non-linear equations, and hence quite different deformed states may correspond to the same load. The number of steady solutions increases as the load increases, and they may differ considerably. Some equilibrium shapes of the ring or rod are stable, and others are not (see Refs 4,5,7 and the references given there).

Non-linear static solutions for loaded rods were obtained in Refs 8 and 9. By linearizing the complete dynamic equations for rods near possible static states, regions of values of the parameters of the problem for which these states are unstable are obtained. Linearization only gives a set of instabilities and criteria for finding possible shapes of the rod by analysing the most unstable modes. As the instability develops, the linear approximation breaks down, and effects of the interaction of different unstable deformation modes become important. Non-linear interactions lead to localization of bendings and the shape of the ring or rod becomes stabilized. Using the example of twisted rods it was shown,[9-11] that, in the region of bifurcation points, it is possible to carry out a global non-linear analysis of the dynamics of local deformations and the conditions for the shape of rods to be stable using amplitude equations.

The amplitude equations for rods are obtained by reductive perturbation theory methods from the complete three-dimensional dynamic equations of the Kirchhoff non-linear model. Here, the difference between the external stress and its critical value defines the order of smallness of the terms of non-linear perturbation theory and serves as a basis for introducing slow variables when describing different deformation scale levels. Small-amplitude patterns from dents on surfaces of longitudinally and hydrostatically compressed shells were described analytically in Refs 12 and 13 using a similar approach.

Below, using the approach described in Ref. 4 we analyse the change in the shape of a thin flexible ring acted upon by an external hydrostatic pressure. In order to carry out the calculations, we will use the Euler–Bernoulli material equation,[4] according to which the moment of the forces which occur when the ring is corrugated is proportional to the change in the curvature of its middle line.

1. Formulation of the model

We will investigate the plane equilibrium states of an initially circular flexible ring of unit height, under an external hydrostatic pressure. Suppose the axis of the ring is directed along the Oz axis of a Cartesian system of coordinates. In the undeformed the state middle line of the ring has a radius R, and when the shape changes it is described by the curve

$$\mathbf{r}(s) = \big(x(s), y(s), 0\big) \tag{1.1}$$

We will choose the length of the plane curve $\mathbf{r}(s)$ as the parameter s. Then, the unit vector of the tangent to the curve is

$$\boldsymbol{\tau} = \mathrm{d}\mathbf{r}/\mathrm{d}s \tag{1.2}$$

Since, in the bending of a thin ring, the distances between the points of the middle line remain the same in the principal approximation, we have $0 \le s \le 2\pi R$.

We will introduce the unit vector $\mathbf{k} = (0,0,1)$ of the ring axis. Then, the unit vector of the outward normal to the surface of the ring is

$$\mathbf{n} = [\boldsymbol{\tau} \times \mathbf{k}]$$

In the Cosserat approach the configuration of the ring is given by a pair of vector-valued functions $\mathbf{r}(s)$ and $\mathbf{n}(s)$.[4]

We will consider an element of the ring, contained in the circumferential direction between the radius vectors $\mathbf{r}(s+ds)$ and $\mathbf{r}(s)$. The material situated in the region $\tilde{s} \ge s + ds$ is the action on this element of the resulting contact force $\mathbf{q}(s+ds)$ and the contact moment $\mathbf{m}(s+ds) = m(s+ds)\mathbf{k}$, while the material in the region $\tilde{s} \le s$ is a force $-\mathbf{q}(s)$ and a moment $\mathbf{m}(s) = -m(s)\mathbf{k}$. The external pressure is always directed along the normal to the ring surface. This leads to the action of a force $p\mathbf{n}ds$ on the element considered. In the case of an external hydrostatic compression $p < 0$.

When these remarks are taken into account, the equilibrium conditions of the ring reduce to the classical equations[4]

$$\frac{\mathrm{d}\mathbf{q}}{\mathrm{d}s} + p\mathbf{n} = 0, \quad \frac{\mathrm{d}\mathbf{m}}{\mathrm{d}s} + [\boldsymbol{\tau} \times \mathbf{q}] = 0 \tag{1.3}$$

Equations (1.3) are the same for plane-deformed and plane-stressed states of the ring.

The contact force vector $\mathbf{q}(s)$ lies in the xOy plane, and hence can be represented in the form

$$\mathbf{q} = q_n\mathbf{n} + q_\tau\boldsymbol{\tau} \tag{1.4}$$

In order to specify the calculation in more detail, we will use the Euler–Bernoulli-Clebsch material equation,[4] according to which the moment of the forces acting when the ring is corrugated, is proportional to the change in its curvature $\tilde{\kappa}$

$$m = -\gamma\left(\tilde{\kappa} + \frac{1}{R}\right) \tag{1.5}$$

where γ is a coefficient of proportionality. In the linear theory

$$\gamma = \frac{Ed^3}{12\left(1 - \sigma^2\right)} \tag{1.6}$$

where d is the ring thickness, E is Young's modulus and σ is Poisson's ratio. The results of the theory of elasticity are often extended to the elasto-plastic region by formal replacement of Young's modulus by the tangent modulus.[5] We will henceforth consider γ as a phenomenological parameter of the model.

Taking into account Frenet's formulae

$$\frac{d\tau}{ds} = \tilde{\kappa}\mathbf{n}, \quad \frac{d\mathbf{n}}{ds} = -\tilde{\kappa}\tau \tag{1.7}$$

we obtain from relations (1.3) and (1.4) a closed system of differential equations in the functions q_n, q_τ, $\tilde{\kappa}$

$$\frac{dq_\tau}{ds} - q_n\tilde{\kappa} = 0, \quad \frac{dq_n}{ds} + p + q_\tau\tilde{\kappa} = 0, \quad \gamma\frac{d\tilde{\kappa}}{ds} + q_n = 0$$

Hence we can express the shear and tangential forces in terms of the curvature of the cross section of the ring

$$q_n = -\gamma\frac{d\tilde{\kappa}}{ds}, \quad q_\tau = \gamma\left(Q - \frac{\tilde{\kappa}^2}{2}\right)$$

The integration constant Q will be determined later.

The curvature of the middle line of the ring satisfies the equation

$$\frac{d^2\tilde{\kappa}}{ds^2} = Q\tilde{\kappa} - \frac{|p|}{\gamma} - \frac{\tilde{\kappa}^3}{2} \tag{1.8}$$

For the further analysis it is more convenient to use the dimensionless variables

$$\theta = s/R, \quad \kappa = R\tilde{\kappa}, \quad q_0 = R^2Q$$

Then $0 \le \theta \le 2\pi$.

In the dimensionless variables the first integral of Eq. (1.8) takes the form

$$\left(\frac{d\kappa}{d\theta}\right)^2 = q_0\kappa^2 - 2\frac{|p|R^3}{\gamma}\kappa - \frac{\kappa^4}{4} + \frac{l_0}{4} \tag{1.9}$$

where l_0 is one more integration constant.

Analysis shows that physically interesting solutions of Eq. (1.9) are only obtained when the fourth-degree polynomial on the right-hand side of Eq. (1.9) has two real roots a and b and two complex-conjugate roots $c = b_1 + ia_1$ and c^*. The roots of the polynomial and the parameters of Eq. (1.9) are connected by the relations

$$b_1 = -\frac{1}{2}(a+b), \quad l_0 = -ab|c|^2, \quad 4q_0 = \frac{3}{4}(a+b)^2 - a_1^2 - ab \tag{1.10}$$

$$8\frac{R^3|p|}{\gamma} = -(a+b)\left[a_1^2 + \frac{1}{4}(a-b)^2\right] > 0 \tag{1.11}$$

Suppose, to be specific, that $a > b$. Taking relations (1.11) into account we obtain the double inequality

$$b < a < -b$$

from which it follows that the parameter b is always negative. The number a can be both negative and positive.

For the conditions formulated above, the general solution of Eq. (1.9) has the form[14]

$$\kappa = \frac{aB(1 - \mathrm{cn}\chi) + bA(1 + \mathrm{cn}\chi)}{B(1 - \mathrm{cn}\chi) + A(1 + \mathrm{cn}\chi)} \tag{1.12}$$

where

$$\chi = \theta/2g, \quad A^2 = (a - b_1)^2 + a_1^2, \quad B^2 = (b - b_1)^2 + a_1^2, \quad g = (AB)^{-1/2}$$

The modulus k of the Jacobi elliptic functions is given by the expression

$$k^2 = \frac{(a-b)^2 - (A-B)^2}{4AB}, \quad 0 \le k^2 \le 1$$

The curvature of the middle line of the ring must be the same when $\theta = 0$ and $\theta = 2\pi$. This leads to the first limitation, imposed on the parameters of the problem

$$\pi\sqrt{AB} = 4K(k)m \tag{1.13}$$

Here K(k) is the complete elliptic integral of the first kind, and the parameter $m = 2, 3, \ldots$ specifies the number of bulges and hollows in the circumferential direction of the ring.

According to expression (1.12), $\kappa \in [b,a]$. The points at which $\kappa = a$ correspond to the botton of a hollow while the points where $\kappa = b$ define the vertices of the bulges of the corrugated ring.

In the xOy plane the unit vectors $\mathbf{n}$ and $\boldsymbol{\tau}$ can be written in parametric form as follows:

$$\mathbf{n} = (\cos\Phi(\theta), \sin\Phi(\theta)), \quad \boldsymbol{\tau} = (-\sin\Phi(\theta), \cos\Phi(\theta))$$

and hence Frenet's equations (1.7) reduce to an equation for calculating the phase $\Phi(\theta)$

$$d\Phi/d\theta = -\kappa(\theta) \tag{1.14}$$

We have established that, for all the admissible values of the parameters of the problem, the solution of Eq. (1.14)

$$\Phi(\theta) = \left[\frac{AB}{a+b} - \frac{aB+bA}{A+B}\right]\theta - \frac{(A+B)^2}{2\sqrt{AB}(a+b)}\Pi\left(\frac{\theta\sqrt{AB}}{2}, \alpha^2, k\right)$$
$$+2\operatorname{acrtg}\left[\frac{a-b}{2\sqrt{AB}} sd\left(\frac{\theta\sqrt{AB}}{2}, k\right)\right] \tag{1.15}$$

possesses the property $\Phi(0) < \Phi(2\pi)$. Here $\operatorname{sd}(x, k) = \operatorname{sn}(x, k)/dn(x, k)$, $\prod(a, \alpha^2, k)$ is the incomplete elliptic integral of the third kind[14] with modulus k and parameter

$$\alpha^2 = -\frac{(A-B)^2}{4AB}, \quad \alpha^2 < 0$$

The constant, which appears after integration of Eq. (1.14), determines the position of a radial line in the xOy plane, from which the phase $\Phi(\theta)$ is measured. In formula (1.15) the constant of integration is chosen so that $\Phi(\theta = 0) = 0$, and the radial line coincides with the Ox axis of the system of coordinates.

In order for the curve $\mathbf{r}(\theta)$ not to have a loop, the function $\Phi(\theta)$ must obtain an increment of 2π when the variable θ changes from zero to 2π. This requirement leads to the second limitation, imposed on the parameters of the problem:

$$\frac{Ab+Ba}{A+B} + 1 + 2m[\Lambda(\beta, k) - 1] = 0 \tag{1.16}$$

where $\Lambda(\beta,k)$ is the Heuman lambda function[14]

$$\Lambda(\beta, k) = \frac{2}{\pi}[\mathbf{E}(k)F(\beta, k') + \mathbf{K}(k)E(\beta, k') - \mathbf{K}(k)F(\beta, k')]$$
$$\beta = \arcsin\frac{2\sqrt{AB}}{A+B}, \quad k' = \sqrt{1-k^2}$$

$F(\beta,k')$ and $E(\beta,k')$ are incomplete elliptic integrals of the first and second kind with modulus k', and $\mathbf{K}(k)$ and $\mathbf{E}(k)$ are complete elliptic integrals of the first and second kind with modulus k.

Integration of Eqs (1.2) and (1.14) gives the shape of the middle line of the ring

$$x(\theta) = x_0 - R\int_0^\theta \sin\Phi(\theta')d\theta', \quad y(\theta) = y_0 + R\int_0^\theta \cos\Phi(\theta')d\theta'$$

The conditions

$$\int_0^{2\pi} x(\theta)d\theta = 0, \quad \int_0^{2\pi} y(\theta)d\theta = 0$$

define the coordinates of the point of intersection of the ring axis with the xOy plane

$$x_0 = \frac{R}{2\pi}\int_0^{2\pi}\int_0^{\theta}\sin\Phi(\theta')d\theta'd\theta, \quad y_0 = -\frac{R}{2\pi}\int_0^{2\pi}\int_0^{\theta}\cos\Phi(\theta')d\theta'd\theta$$

The approximation of linear theory corresponds to a small change in the curvature of the ring, when the parameters a and b are close to one another and to the curvature of the undeformed ring

$$a = -1 + \varepsilon, \quad b = -1 - \varepsilon; \quad 0 < \varepsilon \ll 1$$

Hence, according to relations (1.10), it follows that $b_1 \approx 1$ and, consequently,

$$c \approx 1 + ia_1, \quad A \approx B \approx \sqrt{4 + a_1^2}$$

Then the modulus of the elliptic functions and the integrals $k \approx 0$. In turn, this leads to the fact that all the govething relations are solvable in terms of elementary functions. Condition (1.13) is satisfied identically in the linear approximation, and limitation (1.16) gives

$$A \approx B \approx \sqrt{4 + a_1^2} = 2m \tag{1.17}$$

In the linear in ε approximation we have for the curvature of the ring and the phase

$$\kappa \approx -1 - \varepsilon \cos m\theta, \quad \Phi \approx \theta + \frac{\varepsilon}{m} \sin m\theta$$

Small-amplitude corrugation of the ring is described by the relation

$$\sqrt{x^2 + y^2} \approx R\left(1 + \frac{\varepsilon \cos m\theta}{m^2 - 1}\right) \tag{1.18}$$

According to relations (1.11) and (1.17), the hollows (1.18) appear in the ring when the external pressure exceeds a threshold value, which satisfies the condition

$$|p|_{\Lambda} = \frac{\gamma\left(m^2 - 1\right)}{R^3} \tag{1.19}$$

If we use approximation (1.6) for γ, the modulus of the threshold pressure (1.19) is identical with the critical load according to the linear theory.[5]

For the distortion of hydrostatically compressed envelopes, configurations have been observed experimentally with both a small and a large number of bulges and hollows on their surfaces.[1,2,5]

In the general case, conditions (1.11), (1.13) and (1.16) form a closed system of equations for calculating the unknown constants a, b and a_1. The parameters of this system are the number of hollows m in the circumferential direction of the ring and the external pressure p.

In view of the considerable non-linearity of the equations, the problem can only be solved using approximate-calculation methods. In the following sections we present the results of calculations based on the conjugate-gradient method.[15]

The equations of the non-linear dynamics of a thin ring when there are considerable bendings are easy to obtain using the existing approach.[8,16] The position of point masses of the ring will be described by the radius vector

$$\mathbf{r}(s, \eta, t) = \mathbf{r}_0(s, t) + \eta \mathbf{n}(s, t)$$

where $\mathbf{r}_0(s, t)=(x(s, t), y(s, t), 0)$ is the middle line, $0 \leq s < 2\pi R$ is its natural parameter, $|\eta| \leq d/2$ and d is the ring thickness. We will write the vector of the normal $\mathbf{n}(s,t)$ and the tangential vector $\boldsymbol{\tau}(s,t)$ to the plane curve $\mathbf{r}_0(s,t)$ in the form

$$\mathbf{n}(s,t) = \left(\cos\Phi(s,t), \sin\Phi(s,t), 0\right)$$
$$\boldsymbol{\tau}(s,t) = \frac{\mathrm{d}\mathbf{r}_0}{\mathrm{d}s} = \left(-\sin\Phi(s,t), \cos\Phi(s,t), 0\right) \tag{1.20}$$

Suppose $\mathbf{f}(s, \eta, t)$ is the density of the contact force per unit area in the cross-section of the ring. Consider an element of the ring situated between the radius vectors $\mathbf{r}_0(s+ds,t)$ and $\mathbf{r}_0(s,t)$. The material in the region $\tilde{s} \geq s$ affects the cross-section of the ring with parameter s of the contact force $\mathbf{q}(s,t)$ and the contact moment of the internal forces $m\mathbf{k}$ about the point $\mathbf{r}_0(s,t)$, which are calculated from the formulae[8,16]

$$\mathbf{q}(s,t) = \int_{-d/2}^{d/2} \mathbf{f}(s,\eta,t)\mathrm{d}\eta, \quad m\mathbf{k} = \int_{-d/2}^{d/2} \eta\left[\mathbf{n}(s,t) \times \mathbf{f}(s,\eta,t)\right]\mathrm{d}\eta, \quad \mathbf{k} = (0,0,1)$$

The hydrostatic pressure $p(t)$ leads to the force $p(t)\mathbf{n}(s, t)ds$, which acts on the selected element of the ring.

For the conditions formulated above, the laws of conservation of momentum and angular momentum for an element of the ring reduce to the equations

$$\rho A \frac{\mathrm{d}^2\mathbf{r}_0}{\mathrm{d}t^2} = p\mathbf{n} + \frac{\mathrm{d}\mathbf{q}}{\mathrm{d}s}, \quad \rho I\left[\mathbf{n} \times \frac{\mathrm{d}^2\mathbf{n}}{\mathrm{d}t^2}\right] = \mathbf{k}\frac{\mathrm{d}m}{\mathrm{d}s} + \left[\frac{\mathrm{d}\mathbf{r}_0}{\mathrm{d}s} \times \mathbf{q}\right]$$

where ρ = const is the density of the material, and A and I are the area and moment of inertia of the cross-section of the ring (for a ring of unit height and constant thickness $A = d$ and $I = d^3/6$. Using formulae (1.4), (1.5) and (1.20), we obtain a closed system of dynamic equations for the fields q_n, q_τ and Φ

$$\rho A \begin{Vmatrix} \mathrm{d}^2\Phi/\mathrm{d}t^2 \\ \left(\mathrm{d}\Phi/\mathrm{d}t\right)^2 \end{Vmatrix} + \begin{Vmatrix} \mathrm{d}/\mathrm{d}s & -\mathrm{d}\Phi/\mathrm{d}s \\ \mathrm{d}\Phi/\mathrm{d}s & \mathrm{d}/\mathrm{d}s \end{Vmatrix} \begin{Vmatrix} \mathrm{d}q_n/\mathrm{d}s + p - q_\tau \mathrm{d}\Phi/\mathrm{d}s \\ \mathrm{d}q_\tau/\mathrm{d}s + q_n \mathrm{d}\Phi/\mathrm{d}s \end{Vmatrix} = \mathbf{0}$$
$$\rho I \frac{\mathrm{d}^2\Phi}{\mathrm{d}t^2} - \gamma\frac{\mathrm{d}^2\Phi}{\mathrm{d}s^2} + q_n = 0 \tag{1.21}$$

As previously, the curvature of the ring $\tilde{\kappa} = -d\Phi/ds$.

In this paper we derive possible equilibrium shapes of the ring. They are expressed in terms of elliptic functions and integrals. The dynamic equations (1.21), linearized in the region of each static solution, are reduced to a non-autonomous system of equations with

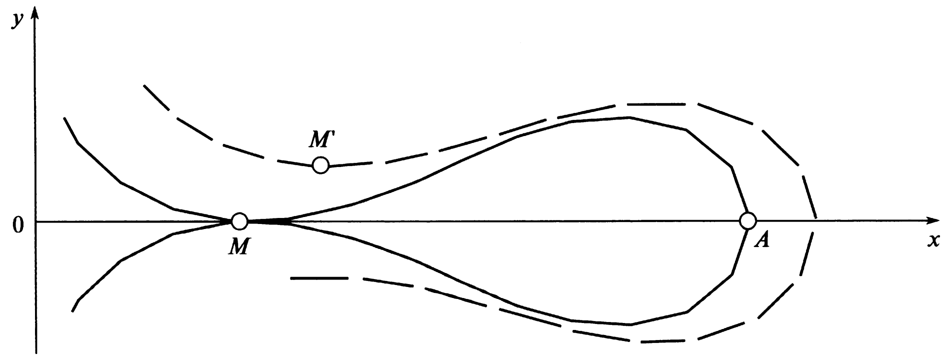

Fig. 1.

coefficients expressed in terms of elliptic functions. An investigation of the spectrum of this problem requires a special analysis. At the same time, the dynamics of the local deformations in the region of the equilibrium shapes of the ring obtained in this paper can be investigated by numerical methods using model (1.21).

2. The change in the shape of the ring under an external hydrostatic compression

Numerical modelling enables us to classify possible types of corrugation of the ring and their relation to the external pressure.

The compressive stresses in the ring material along the directions $\tau(\theta)$ are given by the formula

$$T = \frac{q_\tau}{d} = \frac{\gamma}{dR^2}\left(q_0 - \frac{1}{2}\kappa^2\right)$$

where d is the ring thickness. Calculations showed that the material of the ring experiences maximum compression close to the crests of the bulges:

$$|T|_{\max} = \frac{\gamma}{dR^2}\left|q_0 - \frac{1}{2}b^2\right|$$

The shear stresses along the directions $\mathbf{n}(\theta)$

$$N = \frac{q_n}{d} = -\frac{\gamma}{dR^2}\frac{d\kappa}{d\theta}$$

are a maximum where the second derivative of the curvature vanishes. At these points κ is the root $\kappa_1 \in (b, a)$ of the equation

$$q_0\kappa - \frac{R^3}{\gamma}|p| - \frac{\kappa^3}{2} = 0$$

Hence

$$|N|_{\max} = \frac{\gamma}{2dR^2}\sqrt{(a-\kappa_1)(\kappa_1 - b)}|\kappa_1 - c|$$

The model considered is suitable for analysing changes in the shape of a flexible ring, so long as none of its parts come in contact. When two parts of the ring join together, the nature of their further mechanical interaction must be carefully specified.

We will investigate for what values of $|p|_*$ parts of the ring come in contact. Suppose the Ox axis of a Cartesian system of coordinates passes through the crest A of a bulge, and O is the centre of the ring (Fig. 1). Without loss of generality we can assume that $\theta = 0$ at the point A.

Since the normal $\mathbf{n}$ to the surface of the ring is directed along the Ox axis, the phase function $\Phi(\theta)$ must vanish when $\theta = 0$ (see Eq. (1.14)). In solution (1.15) the integration constant is chosen so that this condition is satisfied.

Suppose parts of the ring touch at the point M, which corresponds to the parameter $\theta = \theta_M$ $(0 < \theta_M < \pi/m)$. In the chosen frame of reference the ordinate of the point M is equal to zero:

$$y(\theta_M) \equiv \int_0^{\theta_M} \cos\Phi(\theta)d\theta = 0 \tag{2.1}$$

and the normal to the middle line of the ring at the point M is parallel to the Oy axis

$$\Phi(\theta_M) = \pi/2 \tag{2.2}$$

Beginning with a certain value of $|p|$, on the middle line of the ring a local minimum occurs at the point M' (see Fig. 1), and the normal $\mathbf{n}(\theta_M)$ is directed parallel to the Oy axis. The parameter θ_M, corresponding to the point M', lies in the section $[\pi/2m, \pi/m]$. The modulus of

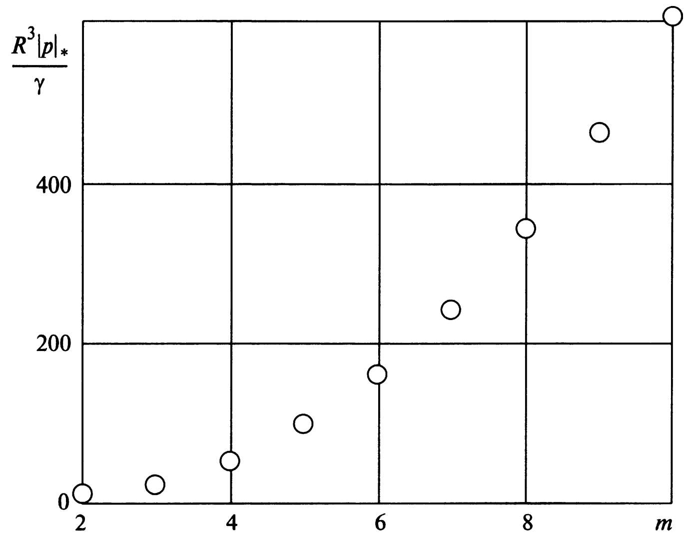

Fig. 2.

the external pressure $|p|$ defines the configuration of the ring continuously, and hence

$$\lim_{|p|\to|p|_*} M' = M$$

In order to obtain the modulus of the limit pressure $|p|_*$, Eq. (2.1) was solved by dividing the section in half. At each iteration it is necessary to solve Eqs (1.11), (1.13) and (1.16) for the unknown parameters a, b and a_1, then obtain θ_M for the configuration defined by the parameters obtained, numerically solve Eq. (2.2) in the section $[\pi/2m, \pi/m]$ for θ_M, and, finally, estimate $y(\theta_{M'})$ using this method.

The dependence of $|p|_*$ on the number of hollows m on the surface of the ring is shown in Fig. 2. The value of $|p|_*$ increases as m increases, and the loop AM narrows. This extends the region of applicability of the model.

The configurations of a deformed ring correspond to the pressures, which satisfy the condition $a = 0$, reminiscent of regular polygons ($m = 3$, see the extreme left part of Fig. 3). Although these dimensionless pressures are close to $R^3|p|_\Lambda/\gamma$, the linear theory does not give the configurations of the type of regular polygons. The formation of plane faces on the surfaces of the hydrostatically compressed shells has been observed experimentally.[2,5]

As the pressure increases the bulges of the ring become more pronounced (see the middle and extreme right part of Fig. 3).

It is important to note that, in the region of the bulges of the deformed ring, the stress intensity may increase so much that plastic flow of the material may begin, and the approximation of the non-linear theory of elasticity will break down. The flow criterion is expressed by the inequality

$$\max[|T|, |N|] \geq \sigma_s$$

where σ_s is the yield point of the material. Numerical calculations show that, at comparatively low pressures, when the corrugation of the ring is small, the stress $|T|$ is greatest. This result agrees with the calculation given in Ref. 3, 17 when discussing the plastic flow of the material of a hydrostatically compressed tube. At the same time, for large bends of the ring we have $|N|_{max} > |T|_{max}$. In other words, plastic flow of the material of shells when there is a considerable corrugation of their surfaces is primarily due to the stress $|N|_{max}$. Graphs of the nondimensional $|N|_{max}$ (the continuous curve) and $|T|_{max}$ (the dashed curve) for $m = 3$ are shown in Fig. 4. Analysis shows that, as the pressure increases, the regions in which the stresses $|N|_{max}$ and $|T|_{max}$ are localized converge. When the local stresses reach the yield point, rigid ribs arise on the side surface of the shell, parallel to the generatrix.[1,2]

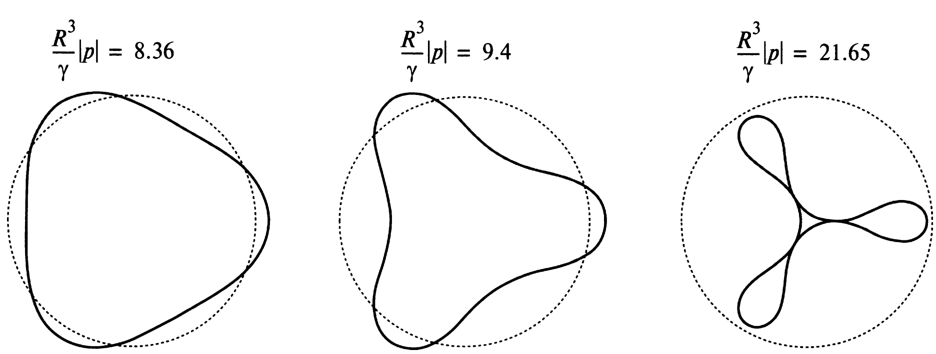

Fig. 3.

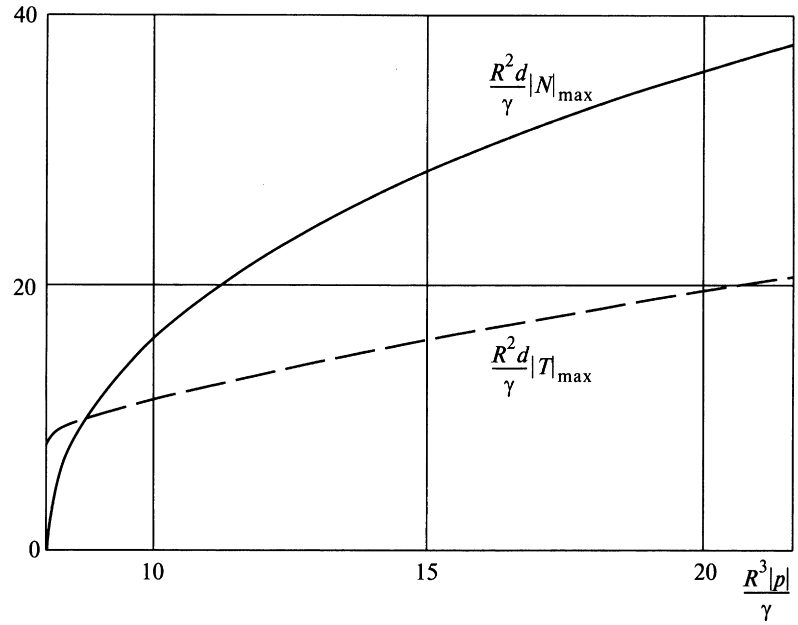

Fig. 4.

3. The change in the shape of the ring on a rigid rod

We will place a rigid rod – mandrel of radius $r < R + d/2$ inside the ring. In Fig. 5a we show the instant of contact between the deformed ring and the rigid rod (the common axis of the ring and the rod passes through the point O). The distance of the curve AB from the crest of the bulge to the bottom of the hollow is equal to $\pi R/m$. Suppose the value $\theta_A = 0$ corresponds to the crest A. Then the natural parameter of the plane curve (1) at the point B is $s_B = \pi R/m$, which corresponds to the dimensionless parameter $\theta_B = \pi/m$.

When the pressure is increased further, the ring begins to bend the rigid rod and takes the form shown Fig. 5b. The point where the ring and the mandrel touch is shifted from position B to position C, where φ is the angle between the radial lines Ox and OC. The natural parameter $s_C = r\varphi + \pi(R-r)/m$ of curve (1) or the dimensionless parameter

$$\theta_C = \eta\varphi + \pi(1-\eta)/m; \quad \eta = r/R$$

corresponds to the point C.

As previously, when calculating the function $\Phi(\theta)$ we choose the integration constant so as to satisfy the condition $\Phi(\theta = 0) = 0$. This choice corresponds to formula (1.15) and its integral representation

$$\Phi(\theta) = -\int_0^\theta \kappa(\theta')d\theta'$$

The procedure for further calculations differs from that discussed previously: the constants, a, b, a_1 and φ are defined by other equations.

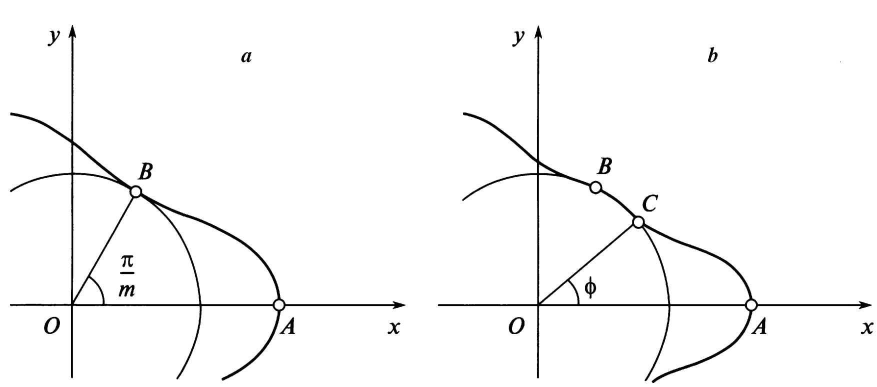

Fig. 5.

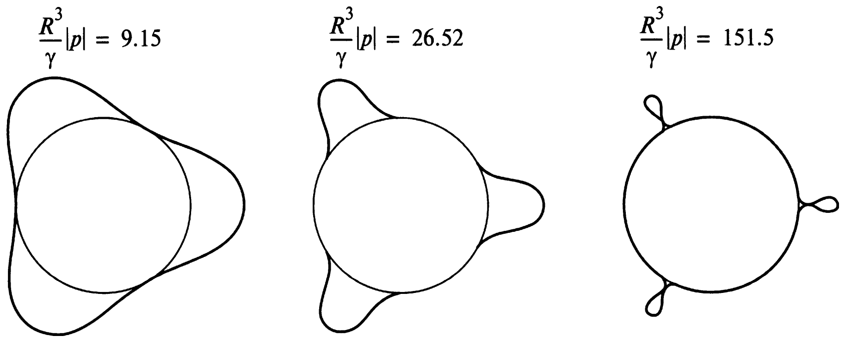

Fig. 6.

From the condition for the tangential vector τ to the surface of the ring to coincide with the tangential vector to the surface of the rigid rod we have

$$-\int_0^{\theta_C} \kappa(\theta')d\theta' = \varphi \tag{3.1}$$

The coordinates of points of the line *AB* are found by integrating Eqs (1.2) and (1.14)

$$x(\theta) = R\int_\theta^{\theta_C} \sin\Phi(\theta')d\theta' + r\cos\varphi, \quad y(\theta) = R\int_0^{\theta} \cos\Phi(\theta')d\theta'$$

At the point where the ring touches the mandrel their coordinates are identical (for simplicity we will neglect the ring thickness). This requirement is equivalent to the equation

$$\int_0^{\theta_C} \cos\Phi(\theta')d\theta' = \eta\sin\varphi \tag{3.2}$$

At the point where the ring envelops the rod, along the direction **n** the external pressure is compensated by the reaction of the mandrel. Hence, in the material of the shell at the point *C* we have

$$q_n = \frac{\gamma}{R^2}\frac{d\kappa}{d\theta}\bigg|_{\theta=\theta_C} = 0$$

In other words, the point *C* corresponds to the minimum of the curvature of curve (1.1): $\kappa(\theta_C) = a$. This leads to the third equation for calculating the parameters of the problem

$$\frac{\pi}{m}(1-\eta) + \eta\varphi = \frac{4K(k)}{\sqrt{AB}} \tag{3.3}$$

Equations (1.11), (3.1), (3.2) and (3.3) define the parameters a, b, a_1 and φ as functions of p and m.

When $\varphi = \pi/m$ conditions (3.1) and (3.3) reduce to governing relations (1.16) and (1.13) for a ring when there is no mandrel. In Fig. 6 we show solutions which illustrate the change in the shape of the ring on a rigid rod for different values of $R^3|p|/\gamma$. The extreme right part of Fig. 6 corresponds to the limiting case.

If the radii of the rod and ring satisfy the relation

$$\pi(R-r) \sim 2md \tag{3.4}$$

the formation of only small-amplitude folds on the ring in a circumferential direction with amplitude $\sim d/2$ is possible. In experimental papers[1,2] usually $m = 3, 4$, according to the change in the shape of the shells. Small-amplitude folds are eliminated during plastic flow of the material, which begins when, as a result of the increase in the external pressure, the stresses heat the crests of the bulges exceed the yield point of the material. Formula (3.4) agrees with experimental data.[1,2]

At the same time, when the difference in the radii of the mandrel and the ring is great, then, as previously, rigid edges are formed on the side surface of the ring (the extreme right part of Fig. 6), which are not removed even when the pressure increases further.

In order to prevent the formation of edges, in the experiments described in Refs 1 and 2, an envelope with an internal rigid rod was placed in a cylindrical container of radius $R_1 > R + d/2$. A reduction in the radius R_1 of the external rigid coupling leads to an increase in the number of waves on the surface of the shell and to a reduction in their amplitude. Small-amplitude waves are completely eliminated after plastic flow of the material occurs. As a result, by hydrostatic compression of tubular blanks, cylindrical articles with variable cross-section along the length were obtained.

4. Conclusion

The proposed model enables us to obtain the relation between the curvature of a deformed ring and the external pressure. From the known curvature, the shape of the ring can be established by methods of differential geometry. Using the model we have theoretically described the initial non-linearly elastic stage of deformation of the ring, connected with the formation of alternating bulges and hollows on the ring in a circumferential direction. At this stage the formation of patterns from the depressions begins at pressures which exceed a certain critical value, and is due to the balance of non-linearity and dispersion effects.

For technological applications it is important that the model should be able to describe theoretically the processes connected with deformation of the ring when there are rigid couplings, which control the number and amplitude of bulges and hollows in a circumferential direction of the ring and prevent the formation of rigid edges on its surface.

We have obtained the equilibrium configurations of the ring that are possible for specified loads and couplings. The use of the energy criterion enables one to separate from the several forms of equilibrium those which can be obtained by a specific method of loading, a specific value of the external pressure, and the material and geometrical parameters of the ring.

A more general way of distinguishing stable ring shapes is to investigate its dynamics in the region of the static solutions obtained. In this paper we have established a model suitable for describing the dynamics of local deformations for considerable bendings of the ring. However, the linearization of the dynamic model in the region of possible equilibrium states of the ring leads to a non-autonomous system of differential equations with coefficients in the form of combinations of elliptic functions. An investigation of the spectrum and the eigenfunctions of the linearized problem is a difficult mathematical problem. In any case, the non-linear dynamics close to bifurcation points and the choice of stable ring shapes can be analysed by numerical methods based on the above model.

References

1. Kamenetskii BI, Taluts GG, Obukhov VA. Investigation of the plastic deformation of cylindrical shells of metal materials by a high-pressure liquid. *Fiz Mat Metaloved* 1996;**81**(3):159–67.
2. Kamenetskii BI, Kiselev VV. Investigation of the plastic deformation of cylindrical shells by a high-pressure liquid. *Kuznechna-Shtampov Proizvod* 2007;**7**:11–7.
3. Hill R. *The Mathematical Theory of Plasticity*. Oxford: Clarendon Press; 1950.
4. Antman S. *Nonlinear Problems of Elasticity*. New York: Springer; 1995, 750p.
5. Vol'mir AS. *The Stability of Elastic Systems*. Moscow: Fizmatgiz; 1963.
6. Lavrent'ev MA, Ishlinskii AYu. Dynamic forms of loss of stability of elastic systems. *Dokl Akad Nauk SSSR* 1949;**64**(6):779–82.
7. Vorovich II. Non-uniqueness and stability in non-linear continuum mechanics. Some mathematical problems. *Uspekhi Mekh* 2006;**4**(1):121–54.
8. Goriely A, Tabor M. Nonlinear dynamics of filaments I. Dynamical instabilities. *Physica D* 1997;**105**(1):20–44.
9. Goriely A, Tabor M. Nonlinear dynamics of filaments II. Nonlinear analysis. *Physica D* 1997;**105**(1):45–61.
10. Lega J, Goriely A. Pulses, fronts and oscillations of an elastic rod. *Physica D* 1999;**132**(3):373–91.
11. Lafortune S, Lega J. Instability of local deformations of an elastic rod. *Physica D* 2003;**182**(1):103–24.
12. Dolgikh DV, Kiselev VV. Dent patterns on the surface of a longitudinally compressed non-linear elastic cylindrical shell. *Prikl Mat Mekh* 2007;**71**(3):500–25.
13. Kiselev VV, Dolgikh DV. A model of the bends of a hydrostaticaly compressed shell close to its stability threshold. *Zh Prikl Mekh Tekh Fiz* 2007;**48**(6):124–34.
14. Byrd PF, Friedman MD. *Handbook of Elliptic Integrals for Engineers and Scientists*. Berlin, etc: Springer; 1971, 378p.
15. Maksimov YuYa, Filippovskaya YeA. *Algorithms for Solving Non-linear Programming Problems*. Moscow: MIFI; 1982.
16. Coleman BD, Dill EH. Flexure waves in elastic rods. *J Acoust Soc America* 1992;**91**(5):2663–73.
17. Kachanov LM. *Fundamentals of the theory of Plasticity*. New York: Dover; 2004.

Translated by R.C.G.